ACS APPLIED MATERIALS & INTERFACES

Research Article

www.acsami.org

Modulating the Activity of Protein Conjugated to Gold Nanoparticles by Site-Directed Orientation and Surface Density of Bound Protein

Feng Liu,[†] Lei Wang,[†] Hongwei Wang,[†] Lin Yuan,*[,†] Jingwen Li,[†] John Law Brash,[‡] and Hong Chen*[,†]

[†]The Key Lab of Health Chemistry and Molecular Diagnosis of Suzhou, College of Chemistry, Chemical Engineering and Materials Science, Soochow University, Suzhou 215123, P. R. China

[‡]School of Biomedical Engineering, Department of Chemical Engineering, McMaster University, Hamilton, Ontario Canada

Supporting Information

ABSTRACT: The key property of protein−nanoparticle conjugates is the bioactivity of the protein. The ability to accurately modulate the activity of protein on the nanoparticles at the interfaces is important in many applications. In the work reported here, modulation of the activity of protein−gold nanoparticle (AuNP) conjugates by specifically orienting the protein and by varying the surface density of the protein was investigated. Different orientations were achieved by introducing cysteine (Cys) residues at specific sites for binding to gold. We chose *Escherichia coli* inorganic pyrophosphatase (PPase) as a model protein and used site-directed mutagenesis to generate two mutant types (MTs) with a single Cys residue on the surface: MT_1 with Cys near the active center and MT_2 with Cys far from the active center. The relative activities of AuNP conjugates with wild type (WT), MT_1, and MT_2 were found to be 44.8%, 68.8%, and 91.2% of native PPase in aqueous solution. Site-directed orientation with the binding site far from the active center thus allowed almost complete preservation of the protein activity. The relative activity of WT and MT_2 conjugates did not change with the surface density of the protein, while that of MT_1 increased significantly with increasing surface density. These results demonstrate that site-directed orientation and surface density can both modulate the activity of proteins conjugated to AuNP and that orientation has a greater effect than density. Furthermore, increasing the surface density of the specifically oriented protein MT_2, while having no significant effect on the specific activity of the protein, still allowed increased protein loading on the AuNP and thus increased the total protein activity. This is of great importance in the study on the interface of protein and nanoparticle and the applications for enzyme immobilization, drug delivery, and biocatalysis.

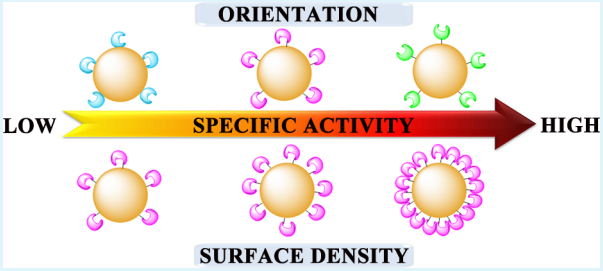

KEYWORDS: *protein, gold nanoparticles, Au−S bond, site-specific orientation, surface density*

1. INTRODUCTION

Protein−nanoparticle conjugates have great potential in many applications of biotechnology, including biocatalysis, biosensors, enzyme immobilization, drug delivery, and bioimaging.[1−5] Gold nanoparticles (AuNPs) are commonly used for protein conjugation because of their good biocompatibility, easily modified chemistry, and high protein loading.[6] The effectiveness of protein−nanoparticle conjugates depends on the activity of the conjugated protein, which should be as close as possible to that of the native state.[7] However, when a protein is conjugated to a AuNP by either covalent or nonspecific interactions, it undergoes some loss of activity in most cases.[8] Factors that modulate the protein activity are various and complex;[9,10] protein orientation and surface density are particularly important.

The correct orientation of a protein conjugated to a nanoparticle is very important for preserving the bioactivity of the protein. If the protein is involved in molecular recognition (e.g., an immunoglobulin or a receptor) and the site that should be recognized by the molecular partner is "hidden" because of the orientation of the protein relative to the solid surface, the recognition process will be compromised.[11] In recent years, a number of methods of controlling the orientation of proteins conjugated to AuNP have been developed. Site-specific methods allow the attachment of proteins with defined orientation where the bioactive site (binding epitope or catalytic site) is freely accessible for interactions required in specific applications.[12] Schiffrin et al. developed thiol-capped AuNP as a building platform.[13] Modification of the ligand shell with nitrilotriacetic acid gave a surface to which histidine-tagged proteins could readily be attached. Brust et al. reported acetylene-functionalized *Thermomyces lanuginosus* lipase-conjugated azide-functionalized water-soluble AuNP that retained the activity of the protein.[14] Chung et al. prepared a DNA oligonucleotide site-specifically coupled to protein G.[15] When used as a linker for immobilization of antibodies to AuNP, a specific orientation

Received: December 1, 2014
Accepted: January 26, 2015
Published: January 26, 2015

DOI: 10.1021/am5084545
ACS Appl. Mater. Interfaces 2015, 7, 3717−3724

of the antibody was achieved with maintenance of the antibody activity.

However, the above methods have limitations, including relatively complex premodification methods and low protein surface density, making it difficult to achieve the required total activity of the protein−AuNP conjugate. With the development of gold−thiol surface chemistry, the Au−S bond has been used increasingly for the preparation of protein−AuNP conjugates. Compared with the above methods, this approach has advantages such as high reaction efficiency, high achievable surface density, and almost no effect of the AuNP size.[16] Hilterhaus et al. reported on glucose-6-phosphate dehydrogenase (G6PDH) with a genetically introduced cysteine (Cys) for site-specific immobilization on AuNP.[17] Two G6PDH variants, one with Cys close to the active center (L218C) and one with Cys far from the active center (D453C), were prepared. The genetically introduced Cys, however, affected the activity of G6PDH. L218C and D453C lost 30−33% of the activity compared to the nonmutated fusion protein. After site-directed immobilization on AuNP, L218C and D453C lost 50% and 89% of the activity of the native enzymes, respectively. Furthermore, the protein surface density was below the saturation level, and the influence of the surface density on the protein activity was not investigated.

The surface density of protein on the nanoparticle will affect its conformational state and therefore its reactivity with target molecules.[8] However, recent studies reported that the effect of the surface density on the protein activity was observed mainly for physically adsorbed protein. Because of the random orientation and weak binding associated with physical adsorption, the protein surface density remains at a relatively low level, even at the saturated state. Siegel et al. reported that 11-nm-diameter AuNP17 lysozyme (Lyz) molecules or 27 α-chymotrypsin (ChT) molecules were adsorbed, and the estimated surface coverage was only 20% and 30%, respectively.[18] As the protein surface density increases, lateral protein−protein interactions will be enhanced and the protein may be reoriented, leading to a loss of activity. It was found that at a saturated state the relative activities of the absorbed ChT and Lyz were only 40% and 20%, respectively. However, Wu et al. showed that Lyz adsorbed on 90-nm-diameter negatively charged silica nanoparticles retained its enzymatic activity only when the surface was close to saturation.[19] Thus, it appears that a further study of the effect of the protein surface density in modulating the protein activity under site-directed orientation is required.

In the work reported here, modulation of the activity of protein−AuNP conjugates by the orientation and surface density was investigated. With *Escherichia coli* inorganic pyrophosphatase (PPase) as a model protein, we used site-directed mutagenesis to generate two mutant types (MTs) with a single Cys residue introduced on the surface (MT_1 with Cys near the active center and MT_2 with Cys far from the active center); the activity of the mutants was found to be the same as that of the wild type (WT). Thus, the mutants were bound to AuNP to give specific orientations via Au−S bond formation, while the WT was bound to the AuNP via physical adsorption. Circular dichroism (CD) was used to measure the conformational changes of the bound protein under different site-specific orientations and surface densities.[20,21] It was shown that the site-directed orientation and surface density can both modulate the protein activity and that orientation has the greater effect. These findings will be beneficial to the study of the biointerface and related applications of protein−nanoparticle conjugates.

2. MATERIALS AND METHODS

Hydrogen tetrachloroaurate hydrate ($HAuCl_4{\cdot}4H_2O$) was purchased from Sinopharm Chemical Reagent Co. (Shanghai, China). Sodium citrate tribasic dehydrate was supplied by Sigma-Aldrich Co. (St. Louis. MO). DNA polymerase (PrimeStar HS), restriction endonucleases, and T_4 DNA ligase were purchased from Takara Biotechnology Co. Oligonucleotides used as the PCR primers were synthesized at Sangon Biotech Co., Ltd. (Shanghai, China). Ellman's reagent [5,5′-dithiobis-(2-nitrobenzoic acid)] was purchased from Sigma Chemical Co. *p*-Chloromercuribenzoate and cysteine (Cys) were purchased from Sangon Biotech Co., Ltd. All aqueous solutions were prepared in 18.2 MΩ·cm purified water from a Milli-Q water purification system (Millipore, Bedford, MA).

Bacterial Strains, Plasmids, and Culture Conditions. The strains of *E. coli* used are as follows: K-12 is a WT strain, and XLI-Blue was used as the host for gene cloning and protein expression. The plasmid pQE30 was used as the vector for production of the native and mutant PPases. The whole *E. coli* strains were grown either in a liquid LB medium (1% Bactotryptone, 0.5% Bacto yeast extract, and 0.5% NaCl, pH 7.0) or on LB plates (1.5% agar).

Cloning of the *ppa* Gene. The polymerase chain reaction (PCR) was used for the cloning of the *ppa* gene encoding the *E. coli* PPase. The chromosomal DNA isolated from *E. coli* K-12 was used as the PCR template. The primers used for the PCR were 5′-CGCGGATCCAGCTTACTCAACGTCCCT-3′ and 5′-CGCAAGCTTTTATTTATTCTTTGCGCGCTC-3′. The PCR product was digested with *Bam*HI and *Hin*dIII and ligated onto the *Bam*HI-*Hin*dIII site of the pQE30 vector. The plasmids were transformed into *E. coli* XLI-Blue, and the transformants containing the *ppa* gene were screened for the production of *E. coli* PPase.

Site-Specific Mutagenesis. Site-specific mutagenesis was performed according to the megaprimer PCR method using Pfu DNA polymerase.[22] In this megaprimer PCR, the forward flanking primer sequence was 5′-CGCAAGCTTTTATTTATTCTTTGCGCGCTC-3′, and the reverse flanking primer sequence was 5′- CGCGGATC-CAGCTTACTCAACGTCCCT-3′. The primer of mutant-type $PPase_1$ used to create K148C-PPase was 5′-CCTCGAAAAAGGCTGCTGGGTGAAAGTTGAAGG-3′ (nucleotides that represent mutations are underlined). The primer of mutant-type $PPase_2$ used to create N124C-PPase was 5′-CACATTAAA-GACGTTTGCGATCTGCCTGAACTGC-3′. The PCR products were then digested with *Bam*HI and *Hin*dIII and ligated onto the *Bam*HI-*Hin*dIII site of the pQE30 vector. DNA sequencing was performed to verify the mutation by Sangon Biotech Co., Ltd.

Expression and Purification. The *E. coli* XLI-Blue cells expressing the WT and mutant PPases were cultured overnight on a shaker at 37 °C and then incubated in a liquid LB medium at 1:100 dilution with shaking at 37 °C until it reached an OD_{600} of 0.5. Isopropyl β-D-1-thiogalactopyranoside (0.5 mM) was added, and the cultures were incubated with shaking at 37 °C for 3 h. The cells were pelleted by centrifugation, and the obtained precipitates were disrupted with Lyz and sonication in 50 mM phosphate buffer (pH 8.0). The cell debris was removed by centrifugation, and then PPase in the supernatant was purified over Ni-NTA Sepharose Resin (Sangon Biotech Co., Ltd.). The purity of the protein was verified by sodium dodecyl sulfate−polyacrylamide gel electrophoresis (SDS-PAGE). The proteins were then purified and concentrated using centrifuge filters (Amicon Millipore with 50 kDa molecular weight cutoff). The purity of the proteins was verified by SDS-PAGE (4% stacking gel and 12% separating gel).

Synthesis of 18-nm-Diameter Citrate-Protected AuNPs. The synthesis of citrate-protected AuNPs followed the reported procedure.[23] To a 250 mL round-bottomed flask equipped with a condenser was added double deionized water (100 mL) and $HAuCl_4$ (12 mM, 516 μL). After the solution reached boiling temperature, sodium citrate (10% w/v, 4.4 mL) was added rapidly with vigorous

DOI: 10.1021/am5084545
ACS Appl. Mater. Interfaces 2015, 7, 3717−3724

stirring, which resulted in a color change from gray to red. Boiling was continued for 10 min, and stirring was continued until the mixture cooled to ambient temperature. It should be noted that all glasses used for the synthesis of AuNPs were washed with an aqua regia solution [3:1 (v/v) HCl/HNO_3] and rinsed thoroughly with double deionized water prior to use.

Conjugation of PPase (WT, MT_1, and MT_2) onto the 18-nm-Diameter Citrate-Protected AuNPs. The solution of 18 nm citrate-protected AuNPs was added to 500 μL of PPase (WT, MT_1, and MT_2) in double deionized water and incubated for 12 h at room temperature, ensuring that CPPase = 0.12 mg mL^{-1} and CPPase/CAuNPs = 60−340. In order to protect the activity of PPase from environmental bacteria, the 1.5 mL EP tubes used in the experiments must be sterilized and the conjugation must be conducted in a sterile environment. For removal of the unbound PPase, PPase-coated particles were centrifuged at 15000*g* four times on an Eppendorf 5804 centrifuge for 20 min and rinsed. The PPase−AuNPs were separated from supernatant and redissolved in 500 μL of deionized water.

Determination of the Free Thiol Content. The free thiol content was determined using Ellman's assay.[24] To prepare the Ellman's reagent solution, Ellman's reagent (4.0 mg, 0.01 mM) was dissolved in 1 mL of sodium phosphate buffer (PB, pH 8.0, 0.1 M) containing 1 mM EDTA. An aliquot of the protein sample (5.0 mg mL^{-1}), 50 μL of an Ellman's reagent solution, and 2.50 mL of PB were mixed for 20 min at room temperature. The absorbance at 412 nm was measured with a Varioskan Flash spectrophotometer (Thermo Scientific, Waltham, MA). The thiol concentration was calculated using the Beer−Lambert law, with a molar extinction coefficient for 2-nitro-5-thiobenzoic acid of 14150 M^{-1} cm^{-1} at 412 nm.

Characterization of PPase−AuNP Bioconjugates. The surface morphology of AuNPs and PPase−AuNP bioconjugates was investigated by transmission electron microscopy (TEM; Hitachi H-600, Tokyo, Japan). Size analysis was performed by dynamic light scattering (DLS) measurements using a Zeta sizer Nano-ZS90 (Malvern Instrument Ltd., Malvern, U.K.) at room temperature. The PPase−AuNP binding was analyzed by spectrophotometry (Varioskan Flash, Thermo Scientific) and SDS-PAGE.

PPase Activity Assay. The catalytic activity of the samples was assayed following the method of Heinonen and Lahti.[25] Enzymatic hydrolysis was performed at 30 °C for 10 min in a 50 mM Tris-HCl buffer (pH 8.0) including 5 μg mL^{-1} PPase, 50 mM $MgCl_2$, and 2 mM inorganic pyrophosphate (PPi). The reaction (total volume of 100 μL) was terminated by the addition of 10 μL of 0.4 M citric acid; then 800 μL of an AAM solution (acetone, 2.5 M sulfuric acid, and 10 mM ammonium molybdate in a 2:1:1 volume proportion) was added to the tubes daily. The contents were mixed, and then 80 μL of citric acid (1 M) was added. The mixed solution was measured with a spectrophotometer at 355 nm. The protein concentration was determined by the Bradford method.[26] The relative amounts of PPase bound to AuNPs (or the conjugates) were calculated by the amount of PPase bound to AuNPs (or the conjugates)/the original amount of PPase in the solution. Also, the relative activity was calculated by the specific activity of PPase−AuNP conjugates/corresponding PPase in aqueous solution.

CD Measurements. CD spectra of the pure PPase and PPase−AuNP bioconjugates were obtained using an AVIV 410 CD spectrometer (AVIV Biomedical, Inc., Lakewood, NJ) using a quartz cuvette with a 0.2 cm path length from 260 to 190 nm at a scan rate of 20 nm min^{-1}. The protein samples were dissolved in double deionized water (final concentration 0.035 mg mL^{-1}). Background scans without protein samples in solution were obtained under the same conditions and subtracted from the wavelength scans prior to converting the angular values to the mean residue molar ellipticity.

3. RESULTS AND DISCUSSION

Chemical Properties of WT Protein and Mutants. To achieve the goal of modulating the protein activity via specific orientation and surface density, a Cys residue was introduced directly at a specific site of the protein using site-directed mutagenesis. As an important protein with no Cys residues on the surface of its three-dimensional structure, PPase catalyzes hydrolysis of PPi into inorganic phosphate in organisms. Thus, PPase was selected as a model protein, and site-directed mutants (MT_1 and MT_2) with a newly introduced Cys residue were built in this study. Lys148 was replaced with Cys in MT_1, while Asn124 was replaced by Cys in MT_2. Lys148 is located in a conserved sequence near the active center in Family I PPases,[27] while Asn124 is on the opposite side of the active center. WT, MT_1, and MT_2 were characterized by SDS-PAGE after protein purification (Figure 1). Bands at 21 kDa appeared in SDS-PAGE for all three mutants, consistent with the expected protein size and indicating that WT, MT_1, and MT_2 were successfully prepared.

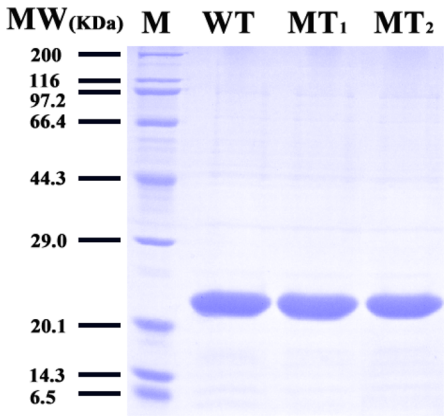

Figure 1. SDS-PAGE of WT, MT_1, and MT_2.

To investigate whether an additional Cys residue was successfully introduced on the surface of MT_1 and MT_2, the free thiol content of the proteins was measured (Table 1). The

Table 1. Chemical Properties of WT, MT_1, and MT_2

protein	mol of free thiol/mol of enzyme	specific activity (kat kg^{-1})
WT	0.036 ± 0.015	8.7 ± 0.2
MT_1	1.086 ± 0.034	9.4 ± 0.2
MT_2	0.944 ± 0.023	8.4 ± 0.1

free thiol content of WT was low, indicating almost no reactive free thiol. This is because two Cys residues in *E. coli* PPase show very low reactivity in the native state; they are buried within the three-dimensional structure of the molecule, making them inaccessible to chemical reagents. In contrast, the free thiol contents of MT_1 and MT_2 were close to 1 mol mol^{-1} protein, indicating that the sulfhydryl group of the Cys residue was accessible. The catalytic mechanism of PPase relies primarily on the lysine, arginine, tyrosine, aspartic acid, and glutamic acid residues in the active center. The Cys residue introduced in MT_1 and MT_2 does not participate in the catalytic reaction, so it may be speculated that the introduction of the Cys residue had little influence on the catalytic activity of the mutants. PPase catalytic activity assay showed MT_1 and MT_2 activities of 9.4 ± 0.2 and 8.4 ± 0.1 kat kg^{-1}, respectively, not significantly different from the 8.7 ± 0.2 kat kg^{-1} value found for WT.

Characterization of AuNP and PPase−AuNP Bioconjugates. AuNPs were prepared by the standard sodium citrate reduction method, and their morphology and size were

DOI: 10.1021/am5084545
ACS Appl. Mater. Interfaces 2015, 7, 3717−3724

determined using TEM and DLS (Figure 2). The TEM data indicated that the AuNPs were well-dispersed, ensuring a high

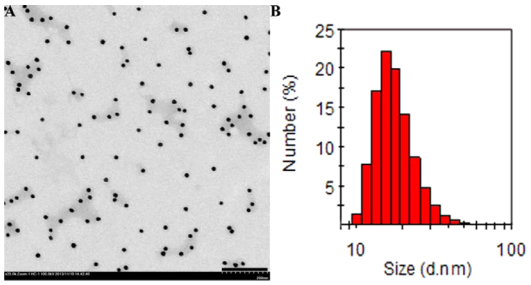

Figure 2. Morphology and size of AuNPs: (A) TEM image (scale bar 200 nm); (B) DLS size distribution.

surface-to-volume ratio in aqueous suspension; this is favorable for the conjugation reactions. The AuNPs were roughly spherical with a diameter of 18 ± 3 nm. The DLS data showed a hydrodynamic diameter of 21 ± 3 nm, with a narrow (virtually uniform) distribution. After conjugation with PPase, the particles changed significantly in morphology and size (Supporting Information, Figure S1). The images confirmed that the proteins were uniformly attached on the surface of the AuNPs, leading to an increase in the diameter of 3−4 nm. The DLS measurements also showed an increase in size after conjugation (Supporting Information, Figure S2). Taken together, these results demonstrate that the different PPases (WT, MT_1, and MT_2) were successfully attached on the surface of the AuNPs.

Protein binding to AuNP induces changes in the absorption spectra of the particles;[28] thus, PPase−AuNP binding was further validated using visible spectroscopy (Figure 3).

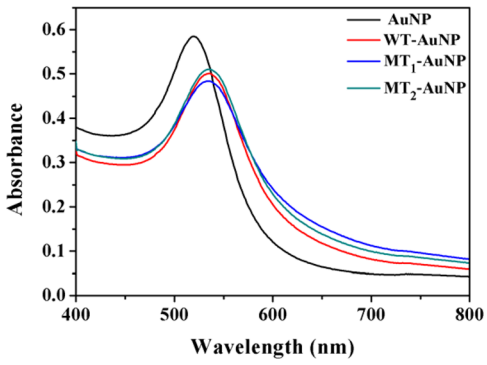

Figure 3. Visible absorption spectra of AuNP in an aqueous suspension.

Compared to the unmodified AuNP, the visible absortion spectra band of PPase−AuNP showed an apparent broadening and red shift. The maximum absorption peak shifted from 522 nm to about 535 nm, indicating the formation of PPase−AuNP conjugates.

For removal of excess unbound PPase after the conjugation reactions, the particles were centrifuged and rinsed several times. The amounts of PPase conjugated to AuNP were estimated by SDS-PAGE (Figure 4). No protein band appeared for the unmodified particles (lane A), and 21 kDa bands appeared for all of the modified particles (lanes B−G), indicating that WT, MT_1, and MT_2 were all successfully conjugated to the AuNP.

The intensities of the protein bands in the gels were used to estimate the relative amounts of PPase attached to the different AuNPs. The data showed that the amounts of MT_1 and MT_2 conjugated to AuNP were higher than that of WT, presumably because there are very few reactive free thiols on the surface of WT, so only small amounts of WT bind to AuNP (probably via physical absorption); MT_1 and MT_2 have about one reactive free thiol per molecule, so they can conjugate to AuNP by Au−S bond formation. For all three mutants, the amounts of protein conjugated to AuNP were obviously higher for CPPase/$CAuNP_2$ than CPPase/$CAuNP_1$; thus, it may be concluded that the amounts of protein conjugated per AuNP can be modulated by controlling the ratio of CPPase/CAuNP. A further study of the effect of the surface density on the protein activity is thus possible.

Modulation of the Protein Activity via Site-Directed Orientation. The correct orientation of the conjugated protein on the nanoparticle is very important to ensure the bioactivity of the protein. An inappropriate orientation will adversely affect the interaction of substrates with the active center. To investigate such effects, the relative activity of the different PPase−AuNP conjugates was measured using samples where the same ratio of CPPase/CAuNP was used in conjugate formation (Figure 5; for specific activity, see Supporting Information, Figure S3). The WT lost about 55% of its activity compared to the native WT; MT_1 lost about 31%, while MT_2 lost only about 9%. From the point of view of orientation, there is no free thiol or other reactive group on the surface of WT; thus, binding of WT to AuNP is presumably by physical adsorption, with random attachment points and no specific orientation. It is also well-known that physical adsorption of protein often results in a conformational change that can result in a loss of activity. The mutants MT_1 and MT_2 can bind to AuNP via Au−S bond formation to give specific site-directed orientations. The Cys residue introduced on MT_1 is near the active center, so this specific orientation affects the interaction of substrates with the protein active center, leading to a loss of activity. However, the substrates are small molecules with relatively little steric hindrance; thus, even when the active center is near the surface of the AuNP, substrates can still access the active center. So, the effect of this site-directed orientation on the protein activity was also limited, and the relative activity of MT_1 still reached about 69%, much higher than that of WT. The Cys residue introduced on MT_2 is far from the active center, so this specific orientation ensures minimal interference with access of substrates and maintains protein activity near the maximum level.

From these considerations, it may be concluded that protein orientation can modulate the protein activity significantly. Compared with randomly oriented protein, protein attached with a specific orientation showed greater activity. The site-directed orientation with its attachment point far from the active center showed very little loss of activity.

Modulation of the Protein Activity via Surface Density. The protein surface density affects the steric hindrance and the conformational state of the protein, which may, in turn, affect the interaction between the substrate and the active center; therefore, the protein surface density also influences the activity. To investigate such effects, the relative activities of PPase−AuNP conjugates were measured under both unsaturated and saturated states (Figure 6A; for specific activity, see Supporting Information, Figure S4). The relative activities of the WT and MT_2 conjugates remained at about

DOI: 10.1021/am5084545
ACS Appl. Mater. Interfaces 2015, 7, 3717−3724

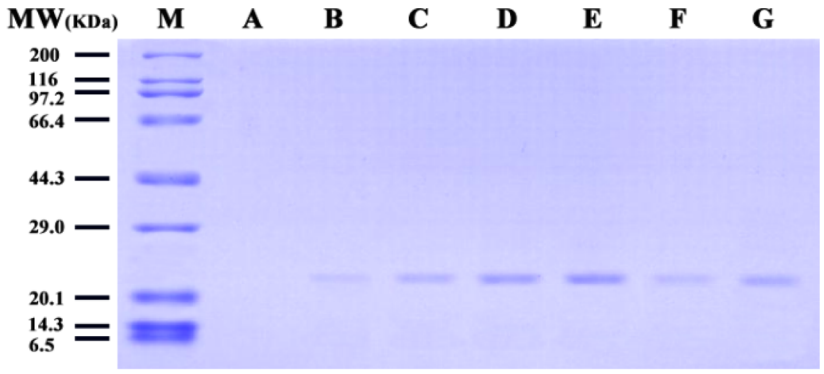

Figure 4. SDS-PAGE of (M) MW markers, (A) unmodified AuNP, (B and C) WT bound to AuNP, (D and E) MT_1 bound to AuNP, and (F and G) MT_2 bound to AuNP. It must be noted that B, D, and F are under the feed molar ratio CPPase/$CAuNPs_1$, while C, E, and G are under the feed molar ratio CPPase/$CAuNPs_2$. CPPase/$CAuNPs_2$ is double CPPase/$CAuNPs_1$.

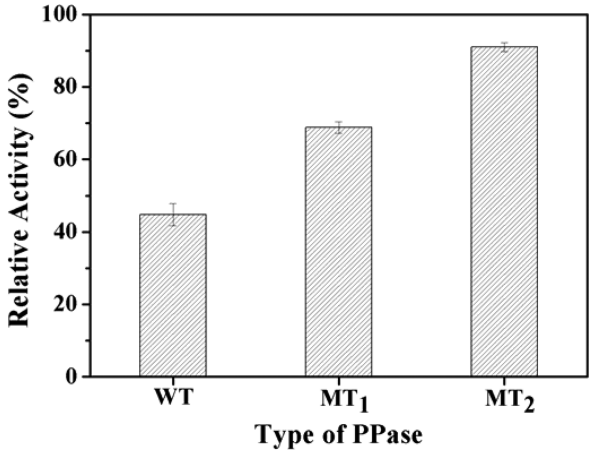

Figure 5. Relative activity of WT, MT_1, and MT_2 on modified AuNP prepared with a PPase/AuNP molar ratio in the feed of 180.

44% and 91% in both unsaturated and saturated states, indicating that the protein surface density did not affect the activity of these materials. For the MT_1 conjugate, the relative activities of the unsaturated and saturated states were significantly different (about 58% and 80%, respectively). To further investigate the effect of the surface density on the protein activity, the activity of PPase−AuNP conjugates over a range of density levels was measured (Figure 6B). The minimum and maximum in the figure refer to the unsaturated and saturated states, respectively. The data showed that the relative activity of the MT_1conjugate increased with increasing protein surface density.

For WT, the protein was most likely bound to the AuNP via weak physical adsorption, giving relatively low protein loading under both the unsaturated and saturated states. Physical adsorption may have resulted in conformational changes of the proteins, leading to losses in the protein activity.[12] So, variation in the surface density could not be used to modulate the activity of the WT conjugate.

For MT_2, PPase is bound to AuNP via Au−S bond formation. The resulting specific orientation maintained the protein activity at its maximum level. The relative activity of the MT_2 conjugate increased only slightly with increasing surface density, so variation of the density could not be used to modulate the activity.

Previous studies demonstrated that the surface density of proteins adsorbed on nanoparticles has an influence on the secondary and tertiary structure of the proteins, and because the activity depends on retention of conformation, the activity is also influenced by the density.[19,29] For MT_1, we speculated that activity modulation by surface density is related to conformational changes in the bound proteins. Therefore, to understand surface density effects, information on conformational change is required.

From the data presented, it is concluded that, for WT and MT_2, the relative activity increased only slightly with increasing surface density. For MT_1, the surface density modulated the

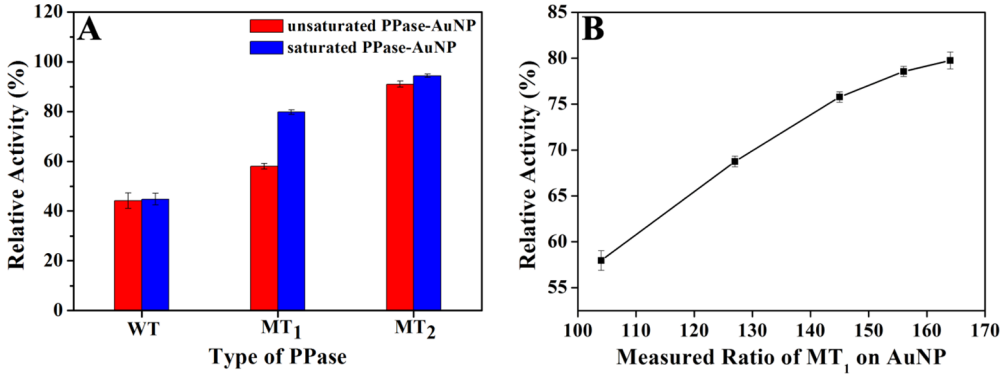

Figure 6. (A) Relative activity of PPase bound to AuNP under unsaturated conditions (PPase/AuNP molar ratio in the feed was 60) and saturated conditions (PPase/AuNP molar ratio in the feed was 400). (B) Relative specific activity of MT_1 bound to AuNP as a function of the feed composition.

DOI: 10.1021/am5084545
ACS Appl. Mater. Interfaces 2015, 7, 3717−3724

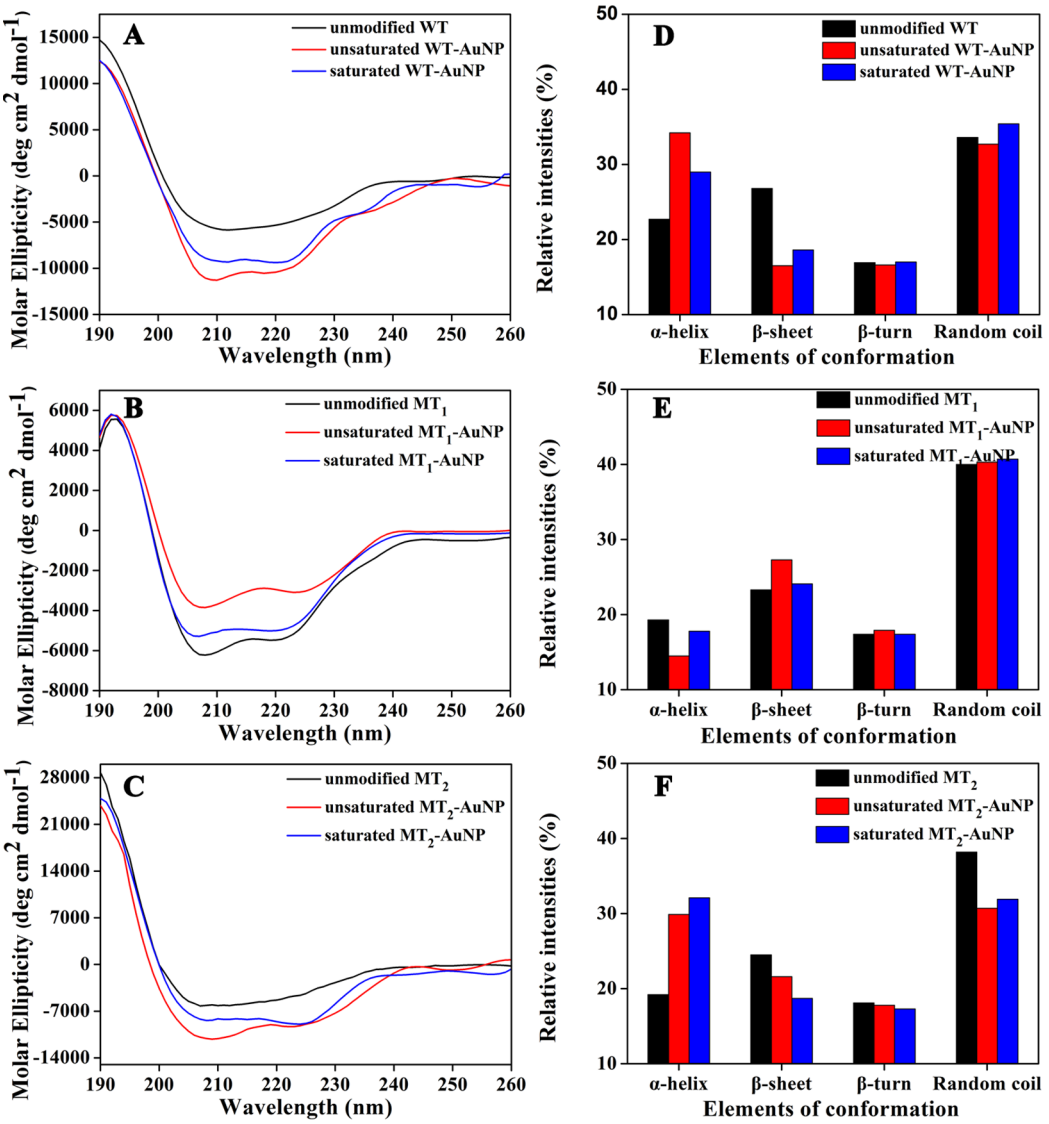

Figure 7. Far-UV CD spectra of PPase−AuNP conjugates (A) WT, (B) MT_1, and (C) MT_2. Relative intensities of conformational elements of (D) WT, (E) MT_1, and (F) MT_2. The black bar is unmodified protein; the red and blue bars are unsaturated and saturated conjugates of the respective PPase. The data were obtained from CD spectra using the CDNN program.

protein activity over a relatively wide range, from 58% to 80%. In general, compared with the surface density, the specific orientation of the protein has a greater effect on the activity.

Influence of Conjugation to AuNP on the Protein Conformation. Previous studies have demonstrated that the interaction of proteins with nanoparticles leads to some conformational change and thus to change in the protein activity.[20,30] To further understand the effects of the specific orientation and surface density on the protein activity, conformational changes for different orientations and surface densities were measured.

CD spectroscopic measurements were performed to evaluate the conformational state of PPase−AuNP conjugates relative to that of the native protein (Figure 7). AuNPs do not exhibit any chiroptical features and are considered to be achiral, as for other unfunctionalized metallic nanoparticles.[31,32] The AuNP substrate thus does not affect CD measurements of PPase−AuNP conjugates.

The CD spectrum of PPase in aqueous solution exhibited two negative bands in the far-UV region (190−250 nm) at 208 and 222 nm, characteristic of the α-helix structure of proteins. The band at 208 nm corresponds to the $\pi \rightarrow \pi^*$ transition of the α-helix, whereas the band at 222 nm corresponds to the $\pi \rightarrow \pi^*$ transition of both the α-helix and random-coil conformations.[33] For the WT and MT_2 conjugates, the intensities of both bands were significantly greater than those of the native PPase, indicating a relative increase in the α-helix content. In contrast, for the MT_1 conjugate, the intensities of both bands decreased in comparison to those of the native PPase, indicating a loss of the α-helix content. In addition, for WT, the intensities of the bands decreased with increasing surface density of the protein; in contrast, for MT_1 and MT_2, the intensities of the bands increased further with increasing surface density of the protein.

The approximate fraction of each secondary structure type could be estimated by assuming the CD spectrum is the sum of fractional multiples of reference spectra for each structural type. In this study, the secondary structural elements of PPase in the native state and in PPase−AuNP bioconjugates were calculated from the CD data using CDNN software.[34] For the WT

DOI: 10.1021/am5084545
ACS Appl. Mater. Interfaces 2015, 7, 3717−3724

conjugate, the content of α-helix increased and that of β-sheet decreased compared to the native state. With an increase of the surface density, the content of α-helix decreased, while that of β-sheet and random coil increased slightly. For the MT_1 conjugate, the content of α-helix decreased and that of β-sheet increased relative to the native state. With an increase of the surface density, the content of α-helix increased and that of β-sheet decreased to the native state value. For the MT_2 conjugate, the content of α-helix increased, while the β-sheet and random coil contents decreased relative to the native state. With an increase of the surface density, the content of α-helix and random coil increased, while that of β-sheet decreased.

For the WT conjugates, the secondary structures changed significantly in both the unsaturated and saturated states, with the transition from β-sheet to α-helix. WT is expected to bind to AuNP via relatively weak physical adsorption, which leads to conformational change of the protein and possibly resulting in a loss of protein activity. For the MT_1 conjugates, the α-helix content decreased, and the β-sheet content increased relative to the native state, but with an increase of the surface density, the secondary structure returned to that of the native state. Thus, it appears that such conformational changes may explain why the activity of the MT_1–AuNP conjugate increased with increasing surface density. For the MT_2 conjugates, the secondary structure changed in both the unsaturated and saturated states. However, protein activities under these two states had no significant difference. This may be because, as the specific orientation in the MT_2 conjugate maintained the active center far from the binding site, the center was "protected" from changes in the secondary structure occurring in locations possibly remote from the center.

4. CONCLUSIONS

In the work reported, the ability of protein–AuNP conjugates to modulate the protein activity depending on the orientation (varied by varying the attachment site on the protein) and surface density of the protein on the particle was studied. It was found using PPase as a model protein that the activity varied widely depending on these two variables. Compared with a randomly oriented protein, protein attached by "site-directed orientation" had greater relative activity, closer to that of the native protein in solution. Site-directed orientation with the attachment site far from the active center allowed virtually complete retention of activity. The surface density did not influence the protein activity for conjugates based on either WT protein or protein attached at a site far from the active center. In contrast, the surface density did influence the activity significantly for conjugates based on protein attached at a site near the active center. Of the two variables, orientation and density, orientation had the larger effect on the protein activity. Furthermore, increasing the surface density of specifically oriented protein allows increased loading of the protein without affecting the activity to any significant extent. The protein activity of the AuNP preparation can thus be increased, which is of great importance in the study on the interface of protein and nanoparticle and the applications for enzyme immobilization, drug delivery, and biocatalysis.

■ ASSOCIATED CONTENT

Supporting Information

Details of TEM images of the AuNP–PPase conjugate, hydrodynamic diameters of AuNP determined by DLS, specific activity of WT, MT_1, and MT_2 in aqueous solution and conjugated to AuNP, and relative protein molecules per AuNP of WT, MT_1, and MT_2 remaining after treatment of the conjugates with SDS. This material is available free of charge via the Internet at http://pubs.acs.org.

■ AUTHOR INFORMATION

Corresponding Authors

*E-mail: yuanl@suda.edu.cn. Tel: +86-512-65880827. Fax: +86-512-65880583.

*E-mail: chenh@suda.edu.cn. Tel: +86-512-65880827. Fax: +86-512-65880583.

Notes

The authors declare no competing financial interest.

■ ACKNOWLEDGMENTS

This work was supported by the National Natural Science Foundation of China (Grants 21334004, 21374070, 21474071, and 21474072), National Science Fund for Distinguished Young Scholars (Grant 21125418), the Priority Academic Program Development of Jiangsu Higher Education Institutions (PAPD), and the Project of Scientific and Technologic Infrastructure of Suzhou (Grant SZS201207).

■ REFERENCES

(1) Chen, Y.-S.; Hong, M.-Y.; Huang, G. S. A Protein Transistor Made of an Antibody Molecule and Two Gold Nanoparticles. *Nat. Nanotechnol.* **2012**, *7*, 197–203.

(2) Ariga, K.; Ji, Q.; Mori, T.; Naito, M.; Yamauchi, Y.; Abe, H.; Hill, J. P. Enzyme Nanoarchitectonics: Organization and Device Application. *Chem. Soc. Rev.* **2013**, *42*, 6322–6345.

(3) Mahmoud, K. A.; Lam, E.; Hrapovic, S.; Luong, J. H. Preparation of Well-Dispersed Gold/Magnetite Nanoparticles Embedded on Cellulose Nanocrystals for Efficient Immobilization of Papain Enzyme. *ACS Appl. Mater. Interfaces* **2013**, *5*, 4978–4985.

(4) Thompson, A. B.; Calhoun, A. K.; Smagghe, B. J.; Stevens, M. D.; Wotkowicz, M. T.; Hatziioannou, V. M.; Bamdad, C. A Gold Nanoparticle Platform for Protein–Protein Interactions and Drug Discovery. *ACS Appl. Mater. Interfaces* **2011**, *3*, 2979–2987.

(5) Zhong, R.; Liu, Y.; Zhang, P.; Liu, J.; Zhao, G.; Zhang, F. Discrete Nanoparticle–BSA Conjugates Manipulated by Hydrophobic Interaction. *ACS Appl. Mater. Interfaces* **2014**, *6*, 19465–19470.

(6) Montalti, M.; Prodi, L.; Zaccheroni, N.; Baxter, R.; Teobaldi, G.; Zerbetto, F. Kinetics of Place-Exchange Reactions of Thiols on Gold Nanoparticles. *Langmuir* **2003**, *19*, 5172–5174.

(7) Secundo, F. Conformational Changes of Enzymes upon Immobilisation. *Chem. Soc. Rev.* **2013**, *42*, 6250–6261.

(8) Shemetov, A. A.; Nabiev, I.; Sukhanova, A. Molecular Interaction of Proteins and Peptides with Nanoparticles. *ACS Nano* **2012**, *6*, 4585–4602.

(9) Zhou, L.; Chen, Z.; Dong, K.; Yin, M.; Ren, J.; Qu, X. DNA-Mediated Construction of Hollow Upconversion Nanoparticles for Protein Harvesting and Near-Infrared Light Triggered Release. *Adv. Mater.* **2014**, *26*, 2424–2430.

(10) Song, Y.; Xu, C.; Wei, W.; Ren, J.; Qu, X. Light Regulation of Peroxidase Activity by Spiropyran Functionalized Carbon Nanotubes Used for Label-Free Colorimetric Detection of Lysozyme. *Chem. Commun.* **2011**, *47*, 9083–9085.

(11) Lynch, I.; Cedervall, T.; Lundqvist, M.; Cabaleiro-Lago, C.; Linse, S.; Dawson, K. A. The Nanoparticle–Protein Complex as a Biological Entity; a Complex Fluids and Surface Science Challenge for the 21st Century. *Adv. Colloid Interface Sci.* **2007**, *134–135*, 167–174.

(12) Wong, L. S.; Khan, F.; Micklefield, J. Selective Covalent Protein Immobilization: Strategies and Applications. *Chem. Rev.* **2009**, *109*, 4025–4053.

(13) Abad, J. M.; Mertens, S. F.; Pita, M.; Fernandez, V. M.; Schiffrin, D. J. Functionalization of Thioctic Acid-Capped Gold Nanoparticles

DOI: 10.1021/am5084545
ACS Appl. Mater. Interfaces 2015, 7, 3717–3724

for Specific Immobilization of Histidine-Tagged Proteins. *J. Am. Chem. Soc.* **2005**, *127*, 5689−5694.
(14) Brennan, J. L.; Hatzakis, N. S.; Tshikhudo, T. R.; Dirvianskyte, N.; Razumas, V.; Patkar, S.; Vind, J.; Svendsen, A.; Nolte, R. J.; Rowan, A. E.; Brust, M. Bionanoconjugation via Click Chemistry: The Creation of Functional Hybrids of Lipases and Gold Nanoparticles. *Bioconjugate Chem.* **2006**, *17*, 1373−1375.
(15) Jung, Y.; Lee, J. M.; Jung, H.; Chung, B. H. Self-Directed and Self-Oriented Immobilization of Antibody by Protein G−DNA Conjugate. *Anal. Chem.* **2007**, *79*, 6534−6541.
(16) Sapsford, K. E.; Algar, W. R.; Berti, L.; Gemmill, K. B.; Casey, B. J.; Oh, E.; Stewart, M. H.; Medintz, I. L. Functionalizing Nanoparticles with Biological Molecules: Developing Chemistries that Facilitate Nanotechnology. *Chem. Rev.* **2013**, *113*, 1904−2074.
(17) Simons, J. R.; Mosisch, M.; Torda, A. E.; Hilterhaus, L. Site Directed Immobilization of Glucose-6-Phosphate Dehydrogenase via Thiol−Disulfide Interchange: Influence on Catalytic Activity of Cysteines Introduced at Different Positions. *J. Biotechnol.* **2013**, *167*, 1−7.
(18) Gagner, J. E.; Lopez, M. D.; Dordick, J. S.; Siegel, R. W. Effect of Gold Nanoparticle Morphology on Adsorbed Protein Structure and Function. *Biomaterials* **2011**, *32*, 7241−7252.
(19) Wu, X.; Narsimhan, G. Effect of Surface Concentration on Secondary and Tertiary Conformational Changes of Lysozyme Adsorbed on Silica Nanoparticles. *Biochim. Biophys. Acta* **2008**, *1784*, 1694−1701.
(20) Roach, P.; Farrar, D.; Perry, C. C. Surface Tailoring for Controlled Protein Adsorption: Effect of Topography at the Nanometer Scale and Chemistry. *J. Am. Chem. Soc.* **2006**, *128*, 3939−3945.
(21) Tsai, D. H.; Delrio, F. W.; Keene, A. M.; Tyner, K. M.; Maccuspie, R. I.; Cho, T. J.; Zachariah, M. R.; Hackley, V. A. Adsorption and Conformation of Serum Albumin Protein on Gold nanoparticles Investigated Using Dimensional Measurements and in Situ Spectroscopic Methods. *Langmuir* **2011**, *27*, 2464−2477.
(22) Li, X.; Wang, L.; Chen, G.; Haddleton, D. M.; Chen, H. Visible Light Induced Fast Synthesis of Protein−Polymer Conjugates: Controllable Polymerization and Protein Activity. *Chem. Commun.* **2014**, *50*, 6506−6508.
(23) Grabar, K. C.; Freeman, R. G.; Hommer, M. B.; Natan, M. J. Preparation and Characterization of Au Colloid Monolayers. *Anal. Chem.* **1995**, *67*, 735−743.
(24) Ellman, G. L. Tissue Sulfhydryl Groups. *Arch. Biochem. Biophys.* **1959**, *82*, 70−77.
(25) Heinonen, J. K.; Lahti, R. J. A New and Convenient Colorimetric Determination of Inorganic Orthophosphate and Its Application to the Assay of Inorganic Pyrophosphatase. *Anal. Biochem.* **1981**, *113*, 313−317.
(26) Bradford, M. M. A Rapid and Sensitive Method for the Quantitation of Microgram Quantities of Protein Utilizing the Principle of Protein−Dye Binding. *Anal. Biochem.* **1976**, *72*, 248−254.
(27) Lahti, R.; Kolakowski, L. F.; Heinonen, J.; Vihinen, M.; Pohjanoksa, K.; Cooperman, B. S. Conservation of Functional Residues Between Yeast and *E. coli* Inorganic Pyrophosphatases. *Biochim. Biophys. Acta* **1990**, *1038*, 338−345.
(28) Casals, E.; Pfaller, T.; Duschl, A.; Oostingh, G. J.; Puntes, V. Time Evolution of the Nanoparticle Protein Corona. *ACS Nano* **2010**, *4*, 3623−3632.
(29) Kumar, C. V.; Chaudhari, A. Proteins Immobilized at the Galleries of Layered α-Zirconium Phosphate: Structure and Activity Studies. *J. Am. Chem. Soc.* **2000**, *122*, 830−837.
(30) Shao, Q.; Wu, P.; Gu, P.; Xu, X.; Zhang, H.; Cai, C. Electrochemical and Spectroscopic Studies on the Conformational Structure of Hemoglobin Assembled on Gold Nanoparticles. *J. Phys. Chem. B* **2011**, *115*, 8627−8637.
(31) George, J.; Thomas, K. G. Surface Plasmon Coupled Circular Dichroism of Au Nanoparticles on Peptide Nanotubes. *J. Am. Chem. Soc.* **2010**, *132*, 2502−2503.
(32) Shemer, G.; Krichevski, O.; Markovich, G.; Molotsky, T.; Lubitz, I.; Kotlyar, A. B. Chirality of Silver Nanoparticles Synthesized on DNA. *J. Am. Chem. Soc.* **2006**, *128*, 11006−11007.
(33) Bolanos-Garcia, V. M.; Ramos, S.; Castillo, R.; Xicohtencatl-Cortes, J.; Mas-Oliva, J. Monolayers of Apolipoproteins at the Air/Water Interface. *J. Phys. Chem. B* **2001**, *105*, 5757−5765.
(34) Bohm, G.; Muhr, R.; Jaenicke, R. Quantitative Analysis of Protein Far UV Circular Dichroism Spectra by Neural Networks. *Protein Eng.* **1992**, *5*, 191−195.

DOI: 10.1021/am5084545
ACS Appl. Mater. Interfaces 2015, 7, 3717−3724